Structures and Properties of Ternary Blends of Recycled Poly(ethylene terephthalate)/Bisphenol-A Polycarbonate/(E/*n*BA/GMA)

Yong Peng, Weihong Guo, Ping Zhu, Chifei Wu

Polymer Alloy Laboratory, School of Materials Science and Engineering, East China University of Science and Technology, Shanghai 200237, People's Republic of China

Received 10 July 2006; accepted 6 March 2007
DOI 10.1002/app.27348
Published online 28 March 2008 in Wiley InterScience (www.interscience.wiley.com).

ABSTRACT: Recycled poly(ethylene terephthalate)/bisphenol-A polycarbonate/PTW (ethylene, butylacrylate (BA), and glycidylmethacrylate (E/nBA/GMA) terpolymer) were blended in different sequence through low temperature solid state extrusion (LTSSE) was studied. R-PET/PC blends were toughened by PTW, resulting in the improvement of impact strengths. In tensile test, the (PC/PTW)/r-PET blends made by mixing r-PET with the preblend of PC/PTW had noticeable strengthening effect on its tensile properties, which was not impaired by the rubber content due to its strain-hardening occurred following its necking at the constant load. Morphological study by scanning electron microscopy (SEM) was in conformity with the mechanical result. For the (PC/PTW)/r-PET blends, the PC particles were well embedded in the PET matrix and the smooth morphology exhibited. The DSC thermographs for heating and cooling run indicated that the crystallinity of PET rich phase was affected by different blending sequence. In the FTIR test, the different absorption intensity of PC aromatic carbonate carbonyl band was clearly illustrated. The results indicated different blending sequence led to different blending effect. J Appl Polym Sci 109: 483–491, 2008

Key words: poly(ethylene terephthalate); bisphenol-A polycarbonate; mechanical properties; compatiblization; crystallinity

INTRODUCTION

As important engineering plastics, both poly(ethylene terephthalate) (PET) and polycarbonate (PC) have been widely industrialized for many years. Homogeneous PET is popular thermal plastics widely used in manufacturing of commercial products, such as PET soft drink bottles. With an ever-growing market, the amount of post consumer PET is accumulating rapidly and becoming an environmental issue. Crystalline PET has excellent chemical resistance and good electronic properties, and amorphous PC possesses high impact toughness, excellent optical properties, and good dimensional stability. Theoretically, recycling of postconsumer PET by blending with PC can be a value-added technique, through which alloys with property combinations of high impact toughness, good dimensional stability from the PC, and excellent solvent resistance and electronic properties from the PET can be made.

PET/PC blends have been extensively studied over the past two decades.[1–20] Paul, Barlow and their coworkers[1–3] stated that, in melt-mixed PC/PET blends, PC and PET were completely miscible in the amorphous phase for PET-rich compositions (70 wt % of PET), whereas PC-rich blends separated into two amorphous phases showing two glass transitions. By means of differential scanning calorimetry (DSC), dynamic mechanical analysis (DMA), and infrared spectroscopy (IR), Chen and Bireley[4] concluded that PC/PET was immiscible over the whole composition range. The extruder-mixed blends had inhomogeneous phase. Thus, simple molten blending of PET and PC in a mixer most probably produced a phase-separated PET/PC mixture with low mechanical strength. The important issues in PET/PC blending were to improve the compatibility between the PET and PC with a third component. The compatibilizers for PET/PC blends can be divided into two groups: the one is called as homogenous phase compatiblizers,[20–24] which promote the miscibility between two immiscible blends through transesterification.[20] The other is called micro-phase separated compatiblizers.[25–33] To improve the impact properties of the blends, toughening by incorporation of rubber or other elastomers, like SEBS,[31,32] known as microphase separated compatiblizers was often required.

Furthermore, the reactive compatibilizers have been increasingly introduced into blends in the past

Correspondence to: W. H. Guo (guoweihong@ecust.edu.cn).

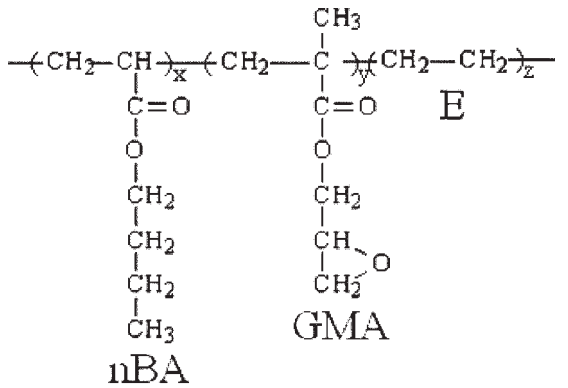

Figure 1 Chemical structure of PTW.

10 years.[24,28,29,31–33] Reactive compatibilization can also provide for a degree of control over morphology development in multiphase polymer blends, via manipulation of the interfacial energies within the system,[34–36] which allowed the formation of a composite dispersed phase during a melt blending process via encapsulation of one dispersed phase by another. With chemical reaction occurring between the functional group and the blends, the interfacial adhesion would be greatly increased and the interfacial tension would be sharply decreased. However, the reactivity between functional groups were different, the way to optimize the compatiblization was needed.

The processing of PET involves hydrolysis and pyrolysis of polymer chain, which reduces not only the intrinsic viscosity and the molecular weight, but also the mechanical properties of recycled materials. Hydrolysis and pyrolysis of PET can be greatly reduced by low temperature solid-state extrusion as the extrusion temperature is between glass transition temperature and cold-crystallization temperature of PET. Modification of recycled PET by low temperature solid state extrusion is an interesting method, it not only provides recycled PET scraps an easy way to recycle by blend processing, but also can form the novel structures such as orientation, crystallization, and the network in the alloy.[37] Therefore, low temperature solid state extrusion is introduced, in which the blending process is performed under high shear strength and low processing temperature to eliminate the influence of pyrolysis and the effect of transesterification.

The effect of blending sequence on the heat properties, morphologies, and mechanical properties with adding the terpolymer consisting of polyethylene, *n*-butyl acrylate (*n*BA) and glycidyl methacrylate (GMA) were studied in this work. The objective of the research project is to further optimize the blending effect of recycled PET and PC for satisfying with the requirement of mechanical properties and acquiring a deeper understanding on the blending and modifying mechanism of the recycled PET and PC in order to facilitate the development of the value-added recycling technique for recycling PET.

EXPERIMENT

Materials and blend preparation

R-PET: Recycled polyethylene terethphalate bottle scraps ($\overline{M_n}$ = 3.85 × 10^4 and $\overline{M_w}$ = 11.9 × 10^4, η = 0.71 dL/g) were purchased from Zijiang Bottle Ltd. (Shanghai, RP China).

PC: Polycarbonate ($\overline{M_n}$ = 20,000) was provided by Teijin Co., Ltd. (Japan).

PTW: Terpolymer of ethylene, butylacrylate (BA) and glycidylmethacrylate (E/nBA/GMA) was supplied by Dupont Co., Ltd (USA), with nominal weight of grafted glycidyl methacrylate = 0.4%. The chemical structure of PTW was shown in Figure 1.

The viscosity versus shear rate curves of r-PET, PC, and PTW were measured at 240°C by Haake rotating rheometer, which was shown in Figure 2. The viscosity of PC is higher than r-PET and PTW. Once blended, PC would be dispersed in the matrix of r-PET and PTW.

r-PET/PC: the blends made by mixing r-PET and PC.

(r-PET/PTW)/PC: the blends made by mixing PC with the preblend of the r-PET/PTW.

r-PET/PTW/PC: the blends made by mixing r-PET, PC, and PTW.

(PC/PTW)/r-PET: the blends made by mixing r-PET with the pre-blend of the PC/PTW.

Prior to blending, recycled PET bottle scraps, and PC pellets were dried at 120°C in a dehumidifying

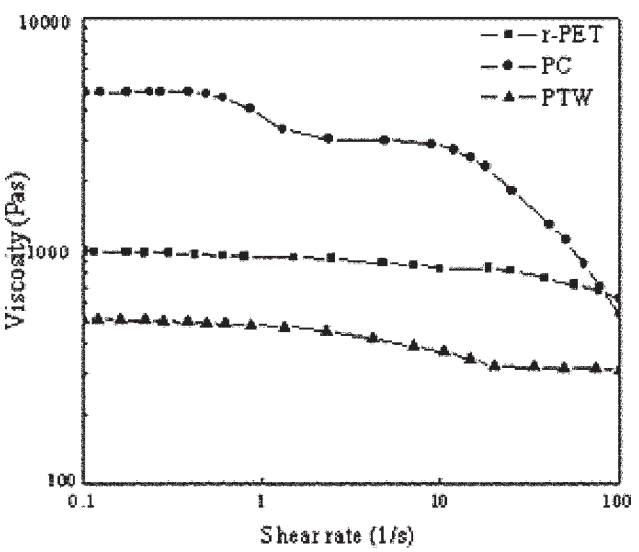

Figure 2 Comparison of melting viscosities at 240°C of r-PET, PC, and PTW.

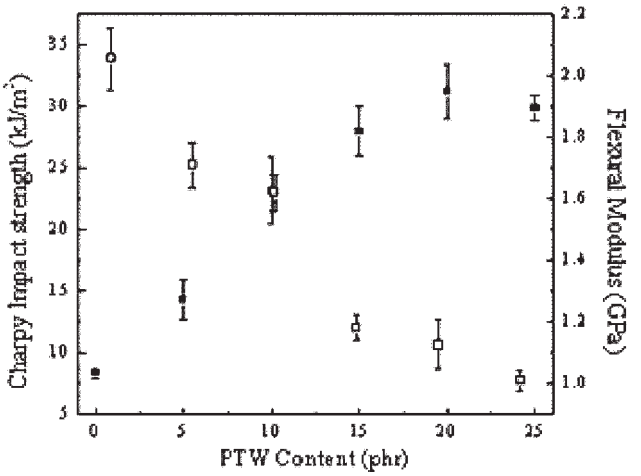

Figure 3 Impact strengths and flexural modulus of r-PET/PC/PTW blends with different PTW content (■-impact strength, □- flexural modulus).

dryer for at least 4 h. PTW was dried in a vacuum dryer for 12 h. Then, the blending was carried out in a co-rotating twin-screw extruder, TEX-30 with Φ = 35 mm, *L/D* = 45 manufactured by Nanjin Ruiya Polymer Machine Co., Ltd (China). Blend components were manually premixed then compounded using a screw speed of 100 rpm, the temperature profile from hopper to die, detailed as 100, 100, 100, 100, 200, 200, 230, and 240°C, respectively. The feeding capacity was kept at 8 kg/h. The blends were extruded as triple laces of 4 mm diameter, which were hauled into a quenching water trough prior to being palletized. Dried blends were molded to form tensile and impact specimens using a QS-100T injection molding machine manufactured by Shanghai Quanshen Polymer Machine Ltd. (China). The barrel temperature profile was set from 190°C (hopper) to 230°C (nozzle) and mold temperature was maintained at 40°C.

Characterization

According to the standard of GB/T1040-1992 (Tensile strength and elongation at break), GB/T9341-2000 (flexural strength and flexural modulus), GB/T1043-1993 (Charpy Impact Strength), the mechanical properties was performed by WSM-20KN universal testing machine by Chang Chun Mechanical Properties Testing Machine Ltd. (China).

The viscosity versus shear rate curves of r-PET, PC, and PTW were measured by Thermo Haake Rheotress 600 rotating rheometer. The measuring temperature was set at 240°C which confirmed with the extrusion temperature.

Differential scanning calorimeter (DSC) was performed on NETZSCH DSC PC 200 (German). Specimens of 10.0 ± 0.2 mg in weight were taken from the core region of injection molded tensile test pieces and was heated from 30 to 280°C at 10°C/min and maintained at 280°C for 5 min to erase the thermal history, and then cooled to 100°C at the speed of −10°C/min in a nitrogen atmosphere.

Attenuated total reflection (ATR) FIIR spectra were performed by using a Bruker Vector 22 instrument with 1 cm^{-1} resolution. The specimens were etched in chloroform to remove PC before being investigated.

Scanning electron microscopy was performed by using a Jeol JSM-35CF (SEM) at accelerating voltage

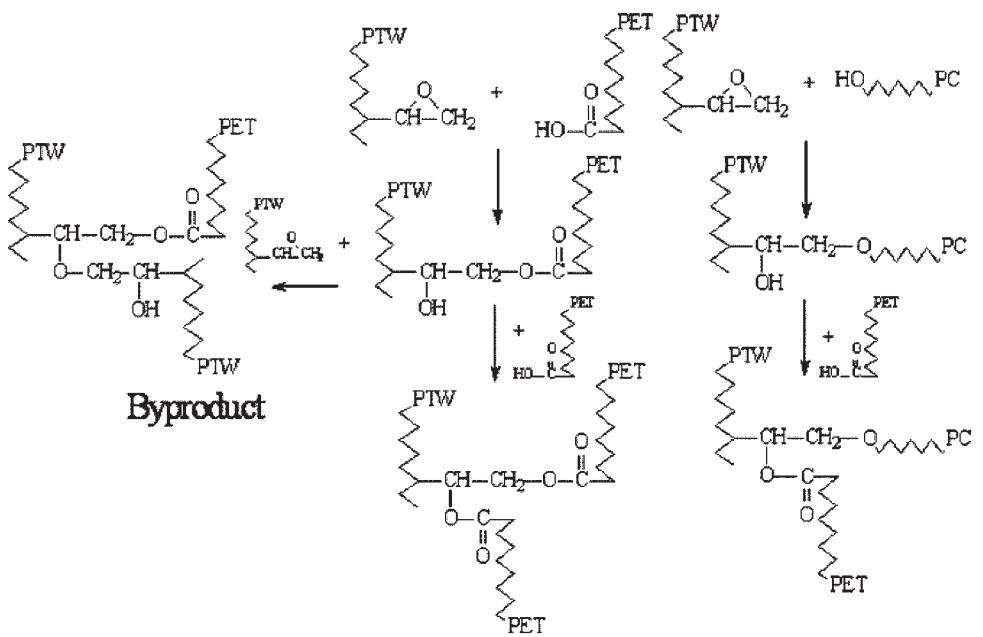

Figure 4 Mechanism for interfacial reaction that occured during reactive blending of r-PET, PC, and PTW.

TABLE I
Mechanical Testing Results of (a) r-PET/PC, (b) (r-PET/PTW)/PC, (c) r-PET/PC/PTW, (d) (PC/PTW)/r-PET

Mechnical properties	a	b	c	d
Impact strength (kJ/m^2)	8.3 (0.4)	20.65 (1.57)	23.11 (1.73)	23.18 (1.99)
Tensile strength at yielding point (MPa)	52.17 (1.21)	41.01 (2.34)	40.09 (1.03)	44.2 (1.45)
Tensile strength at break (MPa)	48.12 (1.78)	36.5 (2.62)	36.94 (0.88)	52.96 (1.32)
Elongation at break (%)	207.2 (2.8)	133.8 (8.6)	220.4 (5.3)	251.9 (5.1)
Flexural strength (MPa)	72.72 (3.5)	55.09 (1.08)	57.79 (1.89)	63.91 (2.66)
Flexural modulus (GPa)	2.055 (0.1)	1.514 (0.065)	1.618 (0.061)	1.777 (0.036)

Sample standard deviations in parentheses.

of 15 kV. All the specimens were impact-fractured at ambient temperature of 25°C, and the fractured surface was gold-coated.

RESULTS AND DISCUSSION

Preliminary test

As the semicrystalline polymers, PET and PC had a high craze stress and modulus; however, with a notch, they nearly all fracture in a brittle manner. It was an efficient way to toughen these materials with incorporation of rubber content. At the same time, these materials will usually be softened with the incorporation of rubber content, which lead to weakening in strengths or modulus. It was important for us to consider the balance between toughness and modulus, and determined the optimum level for further investigation. Figure 3 showed the relationship between toughness and modulus with the PTW content increased from 0 to 25 phr, in which the composition of r-PET/PC was kept at the constant ratio of 75/25. Through the comparison between the impact strengths of the blends with or without PTW, it was showed that the impact strengths increased nearly 300% with the incorporation of PTW (from 8.33 kJ/mol (PTW content = 0 phr) to 31.22 kJ/mol (PTW content = 20phr)). When PTW came to 25 phr, the impact strength was decreased. Thus, it seems that 20 phr content of PTW was the critical point. Otherwise, PTW will be depleted by GMA self-reacting, as shown in Figure 4. And this would bring the effect on the homogeneity of the blends. For binary blends or ternary blends, the properties of material will be greatly influenced by the homogeneity of the blends. Through establishing the relationship between the impact strength and modulus, the content of PTW was chosen at 10 phr for investigating the effect of blending sequence.

Mechanical test

Impact, tensile, and flexural characteristic of the r-PET/PC, the (r-PET/PTW)/PC, the r-PET/PC/PTW, and the (PC/PTW)/r-PET blends were tested and their results were listed in Table I. In the result of impact strengths, a substantial increase in impact toughness was shown with the addition of PTW. The energy dissipated by the rubber content resulted

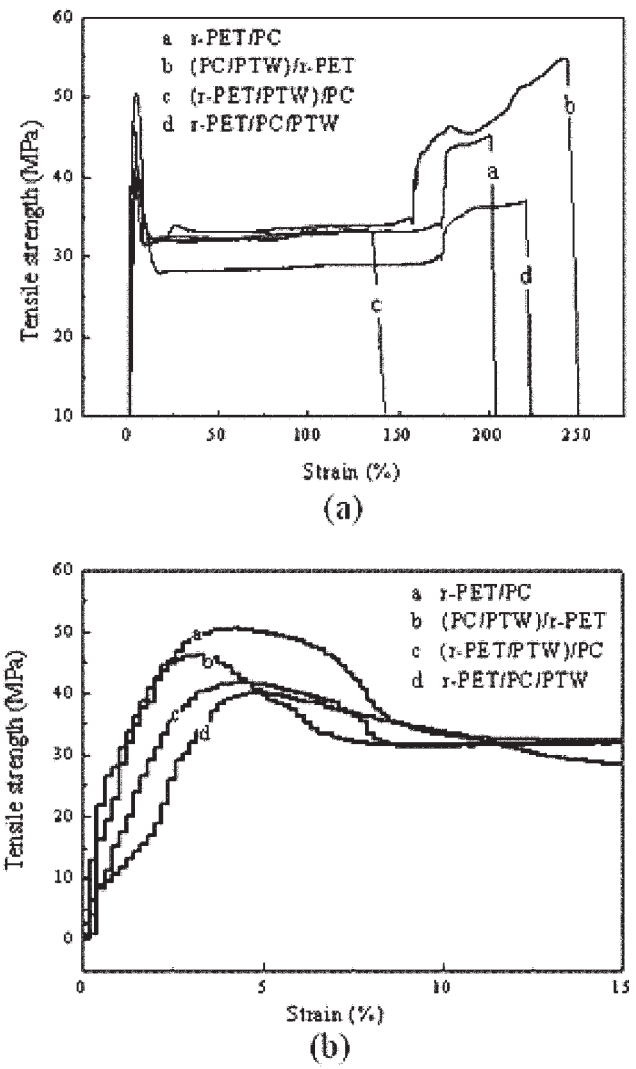

Figure 5 (a) Strain curves of the blends of r-PET/PC, (r-PET/PTW)/PC, r-PET/PC/PTW, and (PC/PTW)/r-PET, (b) Strain curves of the blends of r-PET/PC, (r-PET/PTW)/PC, r-PET/PC/PTW, and (PC/PTW)/r-PET (strain from 0 to 15%).

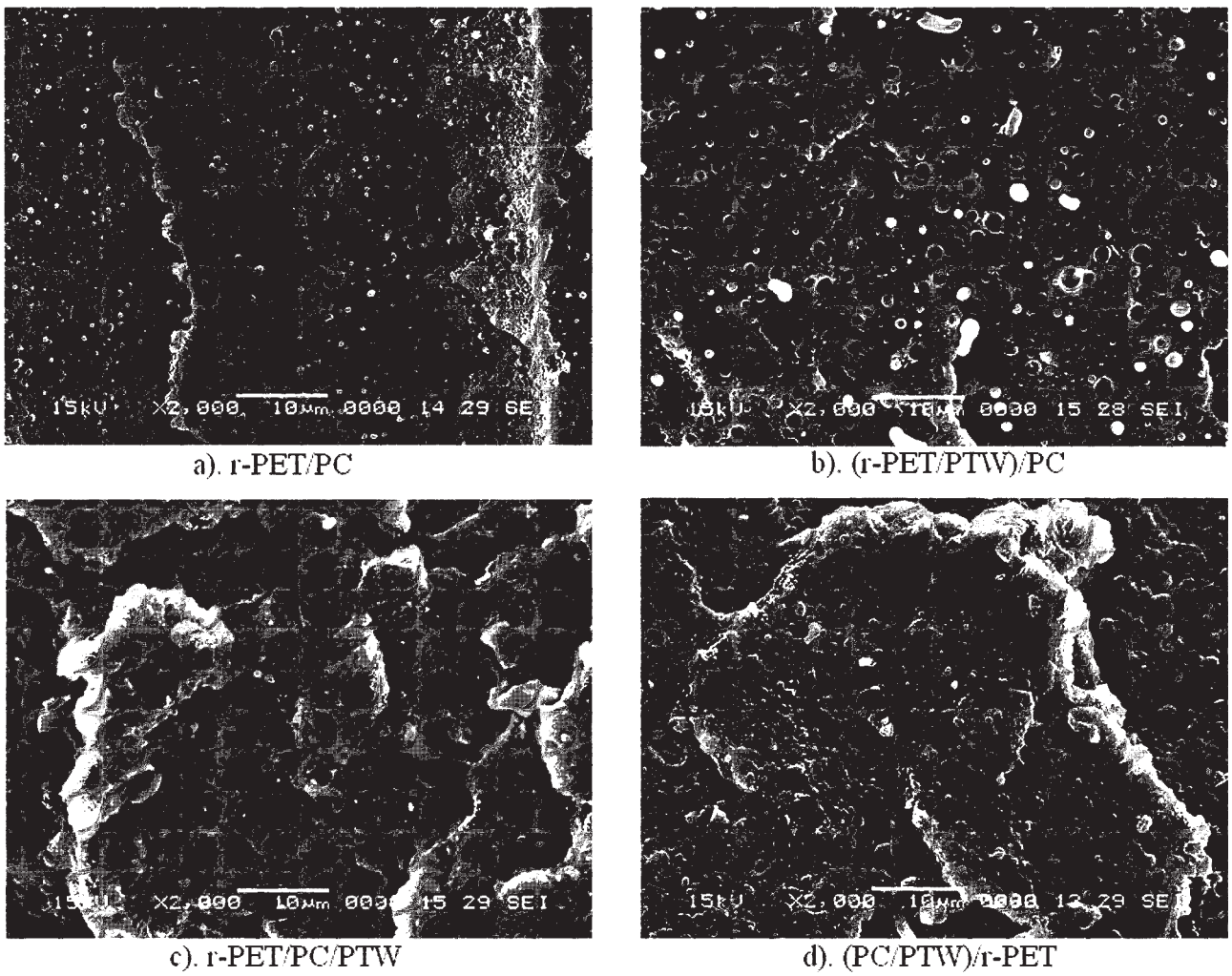

Figure 6 SEM micrographs in low magnification (×2000), (a) r-PET/PC, (b) (r-PET/PTW)/PC, (c) r-PET/PC/PTW, (d) (PC/PTW)/r-PET.

in the increase of impact strengths (from 8.33 kJ/mol to more than 20 kJ/mol). Moreover, (PC/PTW)/r-PET blends had the better impact results than the r-PET/PC/PTW and (r-PET/PTW)/PC blends. However, it is not enough to show the effect of different blending sequence in the impact test. More mechanical tests are needed for further investigation.

From the results of tensile test, the (r-PET/PTW)/PC blends and the r-PET/PC/PTW blends had the loss in their yield strengths. This was caused by rubber content of PTW. However, the situation is different for the (PC/PTW)/r-PET blends which exhibited remarkable tensile properties with much higher tensile strength and elongation shown in Table I. Generally, in the tensile test of semicrystalline thermoplastics, beyond the maximum (the engineering yielding point s_{TY}, where the subscript TY donates tensile yield),[38] they formed a neck. The neck extended in both directions at the constant applied load, until it occupied the whole of the gauge length and meets the shoulders of the specimen. At this point, the load rose; the strain-hardened materials in the neck then extended further and finally broke. Figure 5(a,b) showed the stress–strain curves of the blends made by different blending sequence. For the r-PET/PC/PTW and (r-PET/PTW)/PC blends, their breaks occurred before or at the beginning of strain-hardening, thus, the highest stress was at yielding point, which corresponded with 40.09 and 41.01 Mpa, respectively. Although the r-PET/PC blend broke before its strain-hardening, it has a high value at yielding point which was due to its not added with rubber content. By comparison, the yielding tensile strength of the (PC/PTW)/r-PET blends was only 44.2 Mpa. However, its tensile strength at break has come to 52.96 Mpa, which was due to its further rising load during the strain-hardening and the blends finally exhibited the pronounced tensile property.

The flexural strengths were slightly higher than the tensile strengths. The flexural strengths and

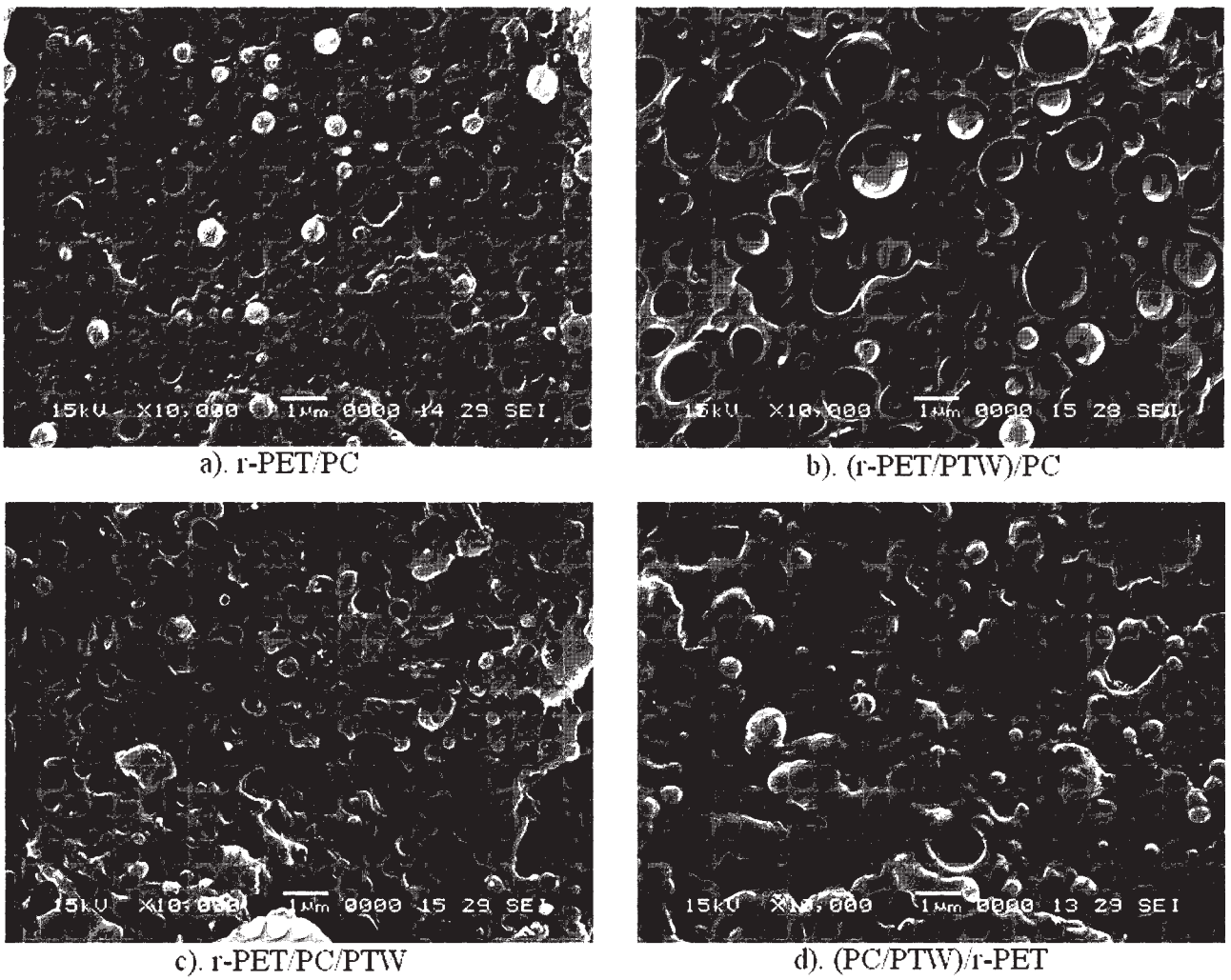

Figure 7 SEM micrographs in high magnification (×10,000), (a) r-PET/PC, (b) (r-PET/PTW)/PC, (c) r-PET/PC/PTW, (d) (PC/PTW)/r-PET.

modulus of the (PC/PTW)/r-PET blend were not as high as that of the r-PET/PC blend, though it is higher than that of the r-PET/PC/PTW and (r-PET/PTW)/PC blends. Generally, injection molding was the preferred method for preparing test samples, levels of molecular orientation were high in the surfaces of both flexural and tensile test bars. However, in flexural test, cracks were necessarily initiated in the outer fiber, where the imposed stresses were at a maximum. By contrast, in tensile samples, the first evidence of crazing and fracture was usually seen in the core region of the molding, where molecular orientation was low. The tensile strengths of the blends were lower than the corresponding flexural strengths. Furthermore, since the yielding behavior of the samples was measured in the flexural test, the flexural strengths corresponded with its yielding behavior. Therefore, the flexural strength of the (PC/PTW)/r-PET blends was not as high as that of the r-PET/PC blends.

Morphology

Modification of PET/PC blends with PTW by low temperature solid state Extrusion was shown in Figure 6(a–d) and Figure 7(a-d). In Figure 6(a), the photomicrographs of the r-PET/PC blends displayed clear phase separation morphology with PC particles (white point) coarsely dispersed in the continuous PET phase, which would attribute to high interfacial tension and poor adhesion between phase boundaries. It was well known that blends based on immiscible polymer pairs were characterized by great interfacial tension which made the dispersion during the blending operation difficult, and contributed to unstable morphology and poor adhesion. The phase distribution of the r-PET/PC/PTW blends and the (PC/PTW)/r-PET blends shown in Figure 6(c,d) was improved by the addition of PTW. However, for the phase of (r-PET/PTW)/PC blends shown in Figure 6(b), the PC particles could be easily identified and the phase boundary seemed to be impaired.

To clearly deserve the morphological difference, SEM micrograph in high magnification (10,000×) was shown in Figure 7(a–d). The r-PET/PC blends had a plain phase with PC particles clearly distinguished. The (r-PET/PTW)/PC blends had the severe phase separation and its particles size was shown to be larger than r-PET/PC. By comparison, the PC particles in the r-PET/PC/PTW and the (PC/PTW)/r-PET blends shown in Figure 7(b,c) were partially or mostly mounted in the PET phase and the adhesion between the phases was greatly improved. Especially for the (PC/PTW)/r-PET blends, in which its PC particles were mostly embedded into the PET matrix, displayed the smooth morphology [shown in Fig. 7(d)]. As a result, the remarkable elongation property and strain hardening behavior of the (PC/PTW)/r-PET blend were mostly due to its stable morphology. By contrast, the poor straining property of the (r-PET/PTW)/PC blend was due to its unstable morphology and poor phase distribution.

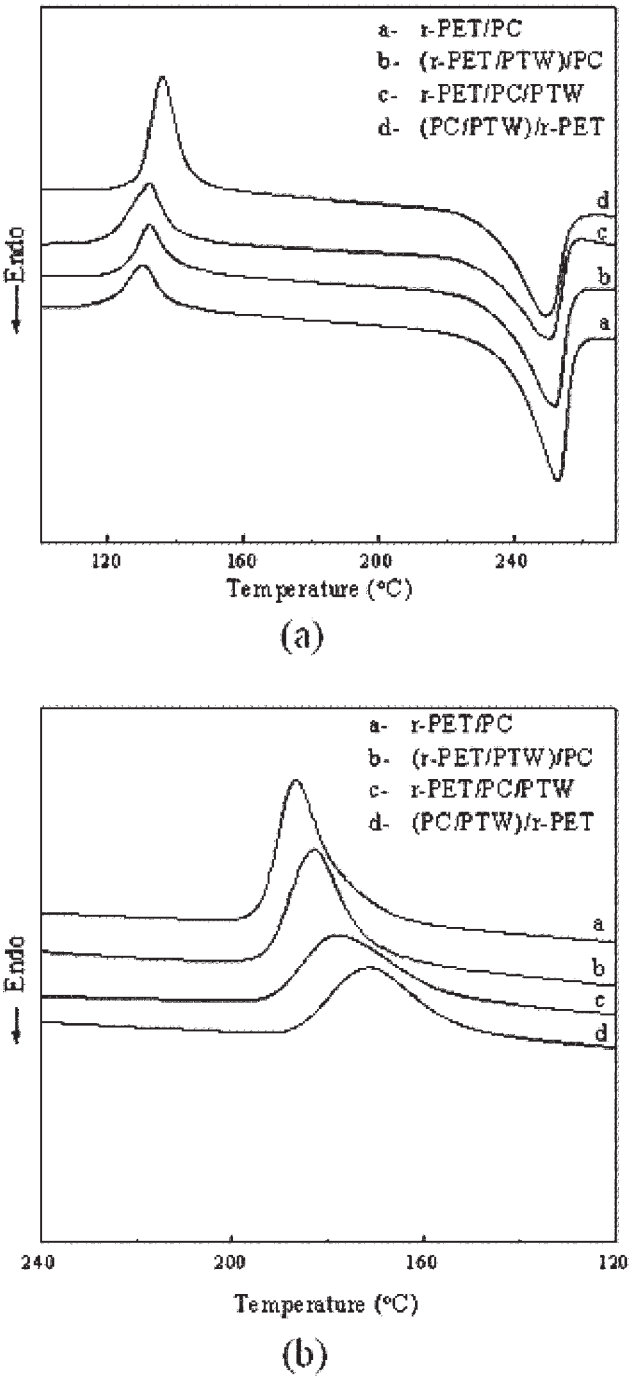

Figure 8 DSC (a) heating and (b) cooling thermographs of the blends of r-PET/PC, (r-PET/PTW)/PC, r-PET/PC/PTW, and (PC/PTW)/r-PET.

Thermal analysis

DSC analysis was made to study the crystallization of PET phase in the blending system. The heating curve was shown in Figure 8(a), which indicated that the cold crystallization temperature (T_{cc}) of PET rich phase increased and melting temperature (T_m) PET rich phase decreased with adding PTW. The corresponding crystallinity was relatively lower than the r-PET/PC blend. From the change of T_{cc}, T_m, and crystallinity of PET rich phase shown in Table II, we expected that the chemical bonding inhibited the crystallization of PET, which lead to increasing in the values of T_{cc} and decreasing in the values of crystallinity.

Furthermore, more detailed data shown in the Table II indicated that crystallization of the samples added with PTW varies with the blending sequence, especially for the blends of (PC/PTW)/r-PET with the much higher value of T_{cc} and the lower value of T_m as compared with blends of r-PET/PC/PTW and (r-PET/PTW)/PC. On the other hand, the trending for areas of cold crystallizing peak and melting peak referred as ΔH_{cc} and ΔH_m were in conformity with that of T_{cc} and T_m.

In the curve of DSC cooling run which was shown in Figure 8(b), the crystallization peak and crystallization temperature T_c of PET was in conformity with the trending in the DSC heating run, which attributed to PET crystallization inhibited by chemical bonding. From the analysis mentioned earlier, we expected that the crystallizing capacity of PET rich phase was (r-PET/PTW)/PC > r-PET/PC/PTW > (PC/PTW)/r-PET. These results implied that the different chemical reaction occurred among PET, PC, and PTW.

FTIR spectrum

Since the epoxy group can react with hydroxyl and carboxyl group, as a reactive compatilizer, PTW would react with PET and PC through reacting with the functional groups mentioned earlier.

TABLE II
Corresponded DSC Data of (a) r-PET/PC, (b) (r-PET/PTW)/PC, (c) r-PET/PC/PTW, (d) (PC/PTW)/r-PET

	T_{cc} (°C)	T_m (°C)	ΔH_{cc} (J/g)	ΔH_m (J/g)	Crystallinity (%)	T_c (°C)	ΔH_c (J/g)	ΔT_c (°C)
a	130.3	253.0	9.10	29.75	14.3	186.7	26.31	66.3
b	131.7	252.0	11.80	26.30	10.0	182.9	23.33	69.1
c	132.2	250.5	12.13	22.83	7.4	176.9	20.16	73.6
d	136.2	249.5	16.34	22.62	4.3	171.4	18.60	78.1

Crystallinity $= \frac{\Delta H_m - \Delta H_{cc}}{\Delta H_m^*} \times 100\%$, in which $\Delta H_m^* = 144.664$ J/g.

Figure 9 showed the FTIR spectrums of r-PET/PC, (r-PET/PTW)/PC, r-PET/PC/PTW, and (PC/PTW)/r-PET blends itched by chloroform to remove PC. 1773 cm^{-1} stretching band representing the PC aromatic carbonate carbonyl band was observed in r-PET/PC/PTW and (PC/PTW)/r-PET blends, which implied that PC was grafted onto PET. By comparison, the absorption peak of 1773 cm^{-1} stretching band was hardly observed in (r-PET/PTW)/PC blend, and only 1720 cm^{-1} stretching band representing the PET aromatic carbonyl band was observed in r-PET/PC blend, which demonstrated that the reaction between PET and PC hardly occurred in these two blends.

Proposed mechanism

(a) r-PET/PC blend: Since PET was almost immiscible with PC, the interaction at the interfacial boundary between PET and PC was weak when they were blended in the twin screw extruder directly. The obvious micro-dispersing morphology of r-PET/PC blend was observed in the Figure 6(a).

(b) (r-PET/PTW)/PC blend: For (r-PET/PTW)/PC blend, it was prepared by mixing the PC with the pre-blend of r-PET/PTW. Since the viscosity of r-PET was close to PTW, the r-PET was dispersed well in PTW and reacted firstly with the epoxy group on PTW. On the other hand, the viscosity of PC was higher than that of r-PET and PTW, it is difficult for PC to disperse well in the r-PET/PTW pre-blend and the reaction between PC and PTW hardly occurred.

(c) r-PET/PC/PTW: It was prepared by mixing r-PET, PC and PTW and the reacting competition between the PET/PTW and PC/PTW occurred. Some PC was grafted onto PET through PTW and the grafted product was located at the interfacial boundary between PET and PC. On the other hand, since the fluidity of PC was lower than that of PET, PET was more likely to react with PTW, which lead to partial PC particles dispersed in the matrix of PET without the transition phase between them.

(d) (PC/PTW)/r-PET: The PC and PTW were preblended and the PC particles would be dispersed into the PTW matrix in the PC/PTW blends before adding r-PET. The PC particles in the PC/PTW blends were well wrap by PTW. When r-PET was mixed with the PC/PTW blends, it is more easily for PTW located between the interfacial boundaries between PET and PC to form the stable morphology and lead to an outstanding strengthening properties exhibited.

CONCLUSION

In this research, PTW played a role of toughening through blending with PET/PC in a series of composition. The composition of r-PET/PC was kept at 75/25 and 10 phr content of PTW was considered as the optimizing formulation by balancing the toughness and modulus. When compared with r-PET/PC/PTW, (r-PET/PTW)/PC blends, the (PC/PTW)/r-PET blends exhibited remarkable tensile and flexural properties. The morphology study revealed that the outstanding tensile behavior of the (PC/PTW)/r-PET blends was due to well embedded PC particles and

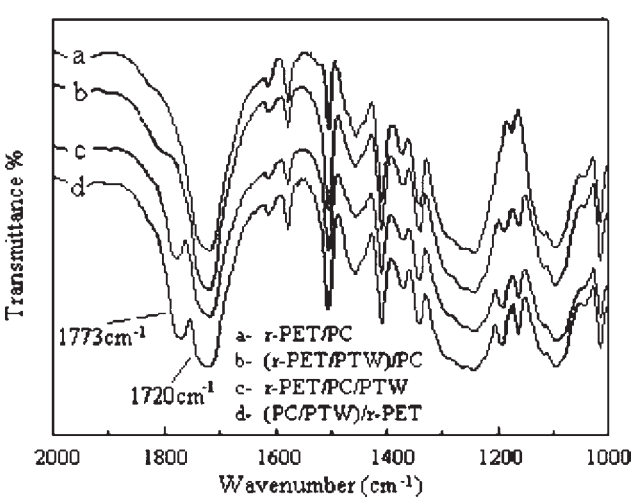

Figure 9 Infrared spectrums of the blends of r-PET/PC, (r-PET/PTW)/PC, r-PET/PC/PTW, and (PC/PTW)/r-PET (Arrows indicated the 1773 and 1720 cm^{-1} band peaks.)

smooth phase morphology in the (PC/PTW)/r-PET blends. From the DSC analysis, the crystallizing capacity of PET rich phase can be expected as (r-PET/PTW)/PC > PET/PC/r-PTW > (PC/PTW)/r-PET. This result indicated that different chemical reaction occurred among PET, PC, and PTW. The FTIR spectrum showed that PC absorption peak was not observed in r-PET/PC blend and the intensities of PC absorption peak were different in the (r-PET/PTW)/PC, r-PET/PC/r-PTW, and (PC/PTW)/r-PET blends.

For the (r-PET/PTW)/PC blends, the preblending of r-PET and PTW was difficult for the high viscosity of PC particles dispersed in the matrix. By comparison, it is more easy for the (PC/PTW)r-PET blends to locate PTW in the interfacial boundaries and to form the stable morphology by preblending PC with PTW and blending PC/PTW blends with r-PET later. As a result, the outstanding strengthening properties of (PC/PTW)/r-PET blend exhibited.

References

1. Nassar, T. R.; Paul, D. R.; Barlow, J. W. J Appl Polym Sci 1979, 23, 85.
2. Barlow, J. W.; Paul, D. R. Polym Eng Sci 1981, 21, 985.
3. Murff, S. R.; Barlow, J. W.; Paul, D. R. J Appl Polym Sci 1984, 29, 3231.
4. Chen, X. Y.; Bireley, A.W. Br Polym J 1985, 17, 347.
5. Pilati, F.; Marianueei, E.; Berti, C. J Appl Polym Sci 1985, 30, 1267.
6. Hanrahan, R. B.; Angeli, S. R.; Runt, J. Polym Bull 1985, 14, 399.
7. Godard, P.; Dekoninck, J. M.; Devisesaver, V.; Devaux, J. J Polym Sci Part A: Polym Chem 1986, 24, 3301.
8. Godard, P.; Dekoninck, J. M.; Devisesaver, V.; Devaux, J. J Polym Sci Part A: Polym Chem 1986, 24, 3315.
9. Hanrahan, R. B.; Angeli, S. R.; Runt, J. Polym Bull 1986, 15, 455.
10. Huang, Z. H.; Wang, L. H. Makromol Chem Rapid Commun 1986, 7, 255.
11. Suzuki, T.; Tanaka, H.; Nishi, H. Polymer 1989, 30, 1287.
12. Wang, L. H.; Huang, Z.; Hong, T.; Porter, R. S. J Macromol Sci Phys B 1990, 29, 155.
13. Berti, C.; Bonora, V.; Fiorina, M.; Pilati, F. Makromol Chem 1992, 193, 1665.
14. Berti, C.; Bonora, V.; Fiorina, M.; Pilati, F. Makromol Chem 1992, 193, 1679.
15. Tan, Q.; Ma, D. Z. J Appl Poly Sci 1993, 48, 747.
16. Zheng, W. G.; Wan, Z. H.; Qi, Z. N.; Wang, F. S. Polym Int 1994, 34, 301.
17. Zheng, W. G.; Wan, Z. H.; Qi, Z. N.; Wang, F. S. Polym Int 1994, 34, 307.
18. Ignatov, V. N.; Carrato, C.; Tartari, V.; Pippa, R.; Scapin, M.; Pilati, F.; Berti, C.; Toselli, M.; Fiorini, M. Polymer 1997, 38, 195.
19. Ignatov, V.N.; Carrato, C.; Tartari, V.; Pippa, R.; Scapin, M.; Pilati, F.; Berti, C.; Toselli, M.; Fiorini, M. Polymer 1997, 38, 201.
20. Guo, Y. Z.; Jing, M. W.; Cui, B. X.; Xiao, L. L.; De, Z. M. Macromol Chem Phys 2001, 202, 604.
21. Kwei, T. K.; Frisch, H. L.; Radogan, W.; Vogel, S. Mocromolecules 1977, 10, 157.
22. Bhatia, Q. S.; Pan, D. H.; Koberstein, J.T. Macromolecules 1988, 21, 2166.
23. Hobbs, S. Y.; Dekkers, M. E. J.; Watkins, H. Polymer 1988, 29, 1598.
24. Machado, J. M.; Lee, C. S. Polym Eng Sci 1994, 34, 59.
25. Eastmond, G. C.; Jiang, M.; Malinconico, M. Polymer 1983, 24, 1162.
26. Tang, T.; Li, L. X.; Huang, B. T. Eur Polym J 1994, 30, 479.
27. Tang, T.; Jing, X. B.; Huang, B. T. J Macromol Sci Phys B 1994, 33, 287.
28. Kim, J. K.; Kim, S.; Park, C. E. Polymer 1997, 38, 2155.
29. Al-Malaika, S.; Kong, W. J Appl Polym Sci 2001, 79, 1401.
30. Hodrokoukes, P.; Floudas, G.; Pispas, S.; Hadjichristidis, N. Macromolecules 2001, 34, 650.
31. Wilkinson, A. N.; Clemens, M. L.; Harding, V. M. Polymer 2004, 45, 5239.
32. Al-Malaika, S.; Kong, W. Polymer 2005, 46, 209.
33. Cheng, T. W.; Keskkula, H.; Paul, D. R. Polymer 1992, 33, 1606.
34. Guo, H. F.; Packirisamy, S.; Gvozdic, N. V.; Meier, D. J. Polymer 1997, 38, 785.
35. Guo, H. F.; Gvozdic, N. V.; Meier, D. J. Polymer 1997, 38, 4915.
36. Reignier, J.; Favis, B. D.; Heuzey, M. C. Polymer 2003, 44, 49.
37. Guo, W. H.; Tang, X. W.; Yin, G. R.; Gao, Y. J.; Wu, C. F. J Appl Polym Sci, unpublished results
38. Paul, D. R.; Bucknall, C. B. Polymer Blends, Vol 2: Performance; Wiley Interscience: New York, 2000.